Biology and Fertility of Soils
https://doi.org/10.1007/s00374-024-01801-4

ORIGINAL PAPER

Lysimeter-based full fertilizer ^{15}N balances corroborate direct dinitrogen emission measurements using the ^{15}N gas flow method

Irina Yankelzon[1] · Lexie Schilling[1,2] · Klaus Butterbach-Bahl[1,3] · Rainer Gasche[1] · Jincheng Han[1] · Lorenz Hartl[4] · Julia Kepp[1] · Amanda Matson[5,6] · Ulrike Ostler[1] · Clemens Scheer[1] · Katrin Schneider[1] · Arne Tenspolde[7] · Reinhard Well[5] · Benjamin Wolf[1] · Nicole Wrage-Moennig[7] · Michael Dannenmann[1]

Received: 19 September 2023 / Revised: 6 February 2024 / Accepted: 7 February 2024

Abstract

The ^{15}N gas flux (^{15}NGF) method allows for direct in situ quantification of dinitrogen (N_2) emissions from soils, but a successful cross-comparison with another method is missing. The objectives of this study were to quantify N_2 emissions of a wheat rotation using the ^{15}NGF method, to compare these N_2 emissions with those obtained from a lysimeter-based ^{15}N fertilizer mass balance approach, and to contextualize N_2 emissions with ^{15}N enrichment of N_2 in soil air. For four sampling periods, fertilizer-derived N_2 losses (^{15}NGF method) were similar to unaccounted fertilizer N fates as obtained from the ^{15}N mass balance approach. Total N_2 emissions (^{15}NGF method) amounted to 21 ± 3 kg N ha^{-1}, with 13 ± 2 kg N ha^{-1} (7.5% of applied fertilizer N) originating from fertilizer. In comparison, the ^{15}N mass balance approach overall indicated fertilizer-derived N_2 emissions of 11%, equivalent to 18 ± 13 kg N ha^{-1}. Nitrous oxide (N_2O) emissions were small (0.15 ± 0.01 kg N ha^{-1} or 0.1% of fertilizer N), resulting in a large mean N_2:($N_2O + N_2$) ratio of 0.94 ± 0.06. Due to the applied drip fertigation, ammonia emissions accounted for < 1% of fertilizer-N, while N leaching was negligible. The temporal variability of N_2 emissions was well explained by the $\delta^{15}N_2$ in soil air down to 50 cm depth. We conclude the ^{15}NGF method provides realistic estimates of field N_2 emissions and should be more widely used to better understand soil N_2 losses. Moreover, combining soil air $\delta^{15}N_2$ measurements with diffusion modeling might be an alternative approach for constraining soil N_2 emissions.

Keywords ^{15}NGF method · Denitrification · N_2 emissions · Nitrogen balance · ^{15}N recovery · NH_3 · N_2O · Drip fertigation

Introduction

Gaseous nitrogen (N) losses from agricultural soils, mainly in form of ammonia (NH_3), and the denitrification products nitrous oxide (N_2O), and dinitrogen (N_2), significantly reduce fertilizer N use efficiency. Despite N_2 emissions represent in most situations the largest gaseous N loss pathway (e.g., Barton et al. 1999; Qasim et al. 2022; Scheer et al. 2020; Zistl-Schlingmann et al. 2019), they are still little constrained. This is because notorious challenges arise by

✉ Michael Dannenmann
michael.dannenmann@kit.edu

[1] Institute for Meteorology and Climate Research, Karlsruhe Institute of Technology, Atmospheric Environmental Research (IMK-IFU), Kreuzeckbahnstrasse 19, 82467 Garmisch-Partenkirchen, Germany

[2] Faculty of Environment and Natural Resources, Chair of Soil Ecology, University of Freiburg, Bertoldstr. 17, 79098 Freiburg i.Br, Germany

[3] Pioneer Center Land-CRAFT, Deptartment Agroecology, University of Aarhus, Aarhus, Denmark

[4] Institut für Pflanzenbau und Pflanzenzüchtung, Bayerische Landesanstalt für Landwirtschaft, Am Gereuth 8, 85354 Freising, Germany

[5] Thünen Institute of Climate-Smart Agriculture, Federal Research Institute for Rural Areas, Forestry and Fisheries, Braunschweig, Germany

[6] Wageningen Environmental Research, Wageningen University and Research, Wageningen, Netherlands

[7] Grassland and Fodder Sciences, Faculty of Agricultural and Environmental Sciences, University of Rostock, 18059 Rostock, Germany

directly measuring soil N_2 emissions due to denitrification in front of high atmospheric background concentrations and atmospheric fluctuations in field studies (Friedl et al. 2020; Groffman et al. 2007). Hence, magnitudes and temporal patterns of denitrification and thus, total N balances, in most terrestrial ecosystems still are not fully understood and accurately constrained (Groffman et al. 2007). Therefore, an improved quantification of soil N_2 emissions is essential to better understand the fates and environmental impacts of reactive N used in agriculture (Galloway and Cowling 2002; Westhoek et al. 2015), including the emissions of the N_2 precursor N_2O, a potent greenhouse gas and ozone-depleting substance (Davidson and Kanter 2014; Ravishankara et al. 2009; Zhang et al. 2023).

Currently, there are basically only two state-of-the-art methods for directly measuring the denitrification products N_2 and N_2O from terrestrial soils as well as their stoichiometry (Friedl et al. 2020; Micucci et al. 2023), the ^{15}NGF and the Helium soil core method. The latter is based on direct N_2 flux measurements in an artificial He-O_2 atmosphere and does therefore not require the addition of an N isotopic tracer that may strongly stimulate denitrification in particular if applied to N-limited ecosystems (Friedl et al. 2020). However, unlike the ^{15}NGF method, the Helium soil core technique is confined to laboratory incubation studies, requiring an exceptionally gas-tight incubation system (Butterbach-Bahl et al. 2002; Cárdenas et al. 2003; Senbayram et al. 2020) to reduce atmospheric N_2 concentration to a few ppmv. It further requires minimal and constant system inherent leakage rates to allow for the quantification of small N_2 fluxes. Solving these challenges requires large engineering efforts and working with larger soil cores leads to substantial He consumption and associated costs.

In contrast to the He-O_2 soil core method, the ^{15}NGF method has been applied in both laboratory and field studies. Large amounts of highly enriched mineral N, typically $^{15}NO_3^-$, are added to the soil, enabling the detection of ^{15}N enrichment not only in N_2O but also in N_2, despite the significant atmospheric N_2 background (Friedl et al. 2020; Mosier and Klemedtsson 1994; Siegel et al. 1982). The fluxes are typically measured by using a static chamber approach, which is based on temporal increases in $^{15}N_2$ headspace gas concentrations over time and subsequent isotopic analysis of gas samples for ^{15}N enrichment in N_2O and N_2 (Friedl et al. 2020; Micucci et al. 2023).

Despite the first field studies on N_2 emissions from fertilized agricultural systems, using the ^{15}NGF, date back to the 1970s, relatively few studies have followed until today, with reported N_2 emissions ranging from 0.4 to 40.2 kg N ha^{-1}, i.e., 0.3–26% of the applied fertilizer N (Baily et al. 2012; Buchen-Tschiskale et al. 2023; Čuhel et al. 2010; Lindau et al. 1990; Liu et al. 2022; Mosier et al. 1989; Pan et al. 2022a; Rolston et al. 1978). It is still unclear to what extent this large variability is driven by different fertilizer types (organic vs. mineral), agricultural systems (e.g., crop vs. grassland), physicochemical soil parameters or climatic conditions, or also by methodological uncertainties.

Major methodological innovation was achieved by Warner et al. (2019), who tested a mobile continuous-flow isotope ratio mass spectrometry (IRMS) system for online in situ measurements of N_2 and N_2O fluxes. Furthermore, Well et al. (2019a) strongly increased the sensitivity of the ^{15}NGF method under field conditions by reducing the ambient N_2 concentration during the chamber measurements through soil flushing with He. Yet, despite being the only method to directly quantify field denitrification rates from upland soils in situ, its use is still relatively limited. This is, probably, due to the high costs associated with isotope additions and the limited availability of delicate analytics, such as isotope ratio mass spectrometry (IRMS) with suitable pre-treatment peripherals, that are required to obtain sufficient sensitivity for $^{15}N_2$ analysis (Galloway and Cowling 2002; Westhoek et al. 2015).

A further challenge is that the method involves a range of inherent uncertainties that are difficult to constrain (Friedl et al. 2020; Micucci et al. 2023), while a successful verification with an alternative and fully independent approach to measuring field N_2 emissions in situ is still missing. There have been a number of studies that compared the N_2 and N_2O fluxes, using the ^{15}NGF method and the acetylene inhibition technique (AIT), respectively (Aulakh et al. 1991; Malone et al. 1998; Mosier et al. 1986a; Sgouridis et al. 2016). Such method comparisons are not promising in view of the widely demonstrated weaknesses of the AIT technique (Butterbach-Bahl et al. 2013). Yang et al. (2011) developed an N_2O labelling-based $^{15}N_2O$ pool dilution method, where gross $^{15}N_2O$ consumption in soil headspace was proposed to equal soil N_2 formation. However, Wen et al. (2016) showed, for various soils, that this approach strongly and irreproducibly underestimates N_2 formation (see also Well and Butterbach-Bahl 2013). A comparison of the ^{15}NGF technique with the He-O_2 soil core technique hitherto also failed to reveal similar results for N_2 emissions (Kulkarni et al. 2014). Furthermore, the He-O_2 soil core technique is not applicable under in situ conditions.

Nitrogen mass balance studies with ^{15}N-labelled fertilizers are a more promising option to constrain gaseous N_2 losses, given that all ^{15}N fates are quantified (plant uptake, soil storage, all gaseous N losses, leaching N losses), so that the unrecovered ^{15}N should equal N_2 losses. Such approaches, however, typically suffer from the huge uncertainty in unrecovered fertilizer ^{15}N that accumulates from the quantification of the numerous N balance components (Micucci et al. 2023; Rolston et al. 1979). This uncertainty

can be reduced by the use of lysimeters. They provide spatially well-constrained setups that are targeted to optimize the accuracy of isotope tracing, N leaching and gaseous N loss measurements (e.g. Kiese et al. 2018; Zistl-Schlingmann et al. 2020). Finally, lysimeters also provide good opportunities to study soil gas concentration changes, which can serve to estimate soil-atmosphere exchange via the gradient method (e.g., Wolf et al. 2011). Interestingly, the latter approach has not yet been used in the context of soil N_2 emissions.

Hence, our objectives were to (1) quantify N_2 emissions and their importance for the fertilizer N mass balance of a winter wheat rotation using the ^{15}NGF method for a quantitative comparison with unrecovered ^{15}N of the ^{15}N fertilizer mass balance approach, and (2) to compare the temporal N_2 emission dynamics at the soil-atmosphere interface by dynamics of ^{15}N enrichment of N_2 in the vertical soil profile in order to assess the potential of soil air $^{15}N_2$ measurements to serve as alternative method to constrain soil N_2 emissions. For this, we cultivated winter wheat on lysimeters, homogenously applied highly ^{15}N enriched mineral fertilizers via drip fertigation at three dates during the cropping period (together 171 kg N ha^{-1}) and analyzed gaseous (NH_3, N_2O, $^{15}N_2$) and hydrological N losses as well as fertilizer N fates in plant and soil, and $^{15}N_2$ enrichment in soil air. Drip fertigation was chosen to achieve homogenous ^{15}N labelling and decrease the role of NH_3 in the N mass balance in favor of N_2. We hypothesized that field N_2 emissions measured by the ^{15}NGF method would be equal to the unrecovered ^{15}N of the total fertilizer ^{15}N mass balance. We further hypothesized that temporal changes in ^{15}N enrichment of N_2 in the soil profile are closely correlated with measured N_2 fluxes at the soil-atmosphere interface.

Materials and methods

Experimental design and lysimeters

To test these hypotheses, we combined a lysimeter experiment with three weighed lysimeters (1 m^2 area each) with a ^{15}N fertilizer tracing experiment over an entire winter wheat cycle. The experimental setup included the determination of N leaching, soil ^{15}N storage and plant ^{15}N export, and the quantification of gaseous N_2O and NH_3 losses to obtain a particularly precise estimate of the unrecovered ^{15}N fertilizer which is related to N_2 losses. Furthermore, we directly quantified soil N_2 emissions with high temporal resolution and for the entire lysimeter areas using the ^{15}NGF method, accompanied by measurements of the dynamics of soil air $^{15}N_2$ enrichment over the entire experimental period.

The lysimeters (Fig. 1) were manufactured according to Pütz et al. (2016) by UGT (Umwelt Geräte Technik, Müncheberg, Germany). The lysimeters were constructed of stainless-steel cylinders with a surface area of 1 m^2 and a depth of 1.5 m. A stainless-steel plate that was tightly bolted to the cylinder served as the cylinder's bottom closure. The lysimeters were filled with intact soil monoliths extracted from an agricultural field close to the town of Bad Rotthalmünster, Germany, on March 27, 2020. On April 1st, 2020, the lysimeters were delivered to the lysimeter field site of Campus Alpin of the Karlsruhe Institute of Technology (IMK-IFU), Garmisch-Partenkirchen (185 km southwest of the soil sampling). The original, undisturbed soil structure was carefully preserved during soil extraction and transport. On April 8, 2020, the installation of the lysimeters was completed. The soil was classified as a Luvisol derived from loess, containing 10% sand, 71% silt, and 19% clay in the ploughing layer. Its pH ($CaCl_2$) was measured to be 6.7 (Rethemeyer 2004; Rohe et al. 2021).

Various sensors and probes were installed at different depths of the lysimeter (Fig. 1). Combined soil moisture/soil temperature sensors (SMT-100, UGT GmbH, Germany) were placed at 10, 20, 30, 50 and 120 cm depths to determine the temperature and volumetric water content of the soil. Soil water content and soil temperature were recorded by data loggers (DT85, DataTaker-Thermo Fisher Scientific Australia Pty Ltd., Scoresby, VIC, Australia) every ten minutes. For soil water sampling, the lysimeters were supplied with suction cups with ceramic tips at the same depths (UGT GmbH, Munich, Germany), in conjunction with a vacuum control unit (VS, UMS, Munich, Germany) operating at 100 hPa. The vacuum was applied on sampling bottles for each sampling depth that collected soil water through the suction cups. For sampling of soil air, custom-made semi-permeable polypropylene membrane (PP V8/2 HF membrane, Accurel®, Akzo Nobel Faser AG, Wuppertal, Germany) gas lances with a nominal pore size of 0.2 µm, inner diameters of 5.5 mm, and lengths of 80 cm were installed horizontally at depths of 10, 20, 30, 50, and 120 cm.

Since a natural hydraulic gradient and water flow would normally be hampered by the closure at the bottom of the lysimeters, a suction rake formed out of six silicon carbide porous cups (SIC40, UMS AG, Munich, Germany) was installed at the lower boundary of the lysimeter (in 140 cm soil depth), to establish in situ hydrological field conditions within the lysimeters. For this, a bidirectional pump was employed to adjust the water content of the lower lysimeter boundary via the suction rake. To maintain consistent water tension both within and outside the lysimeters, water was either extracted from or introduced into them. A tensiometer, specifically the TS1 model (UMS AG, Munich, Germany),

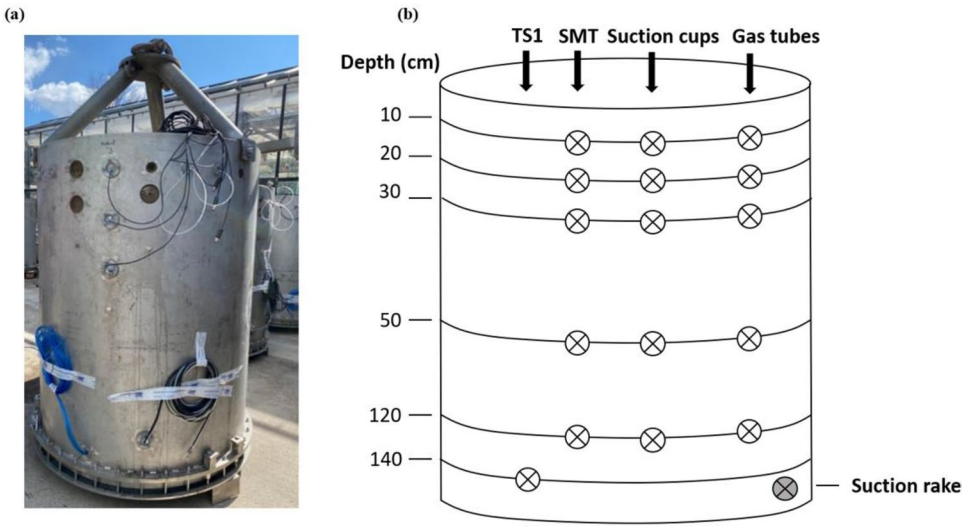

Fig. 1 (**a**) Lysimeter filled with Rotthalmünster soil, equipped with the sensors and tubing, ready for the installation at IMK-IFU. (**b**) Scheme of lysimeter sensor equipment: TS1: tensiometer; SMT: soil moisture/soil temperature probes; Suction cups for water sampling; Gas tubes for soil gas concentration measurements; Suction rake for water exchange at the lower boundary layer between lysimeter and drainage tank

was positioned within the lysimeter at a depth of 140 cm for this purpose. In addition, three reference tensiometers were placed at the same depth outside, in direct vicinity to the lysimeters in the field. Water flow out of or into the lysimeters was adjusted according to the matric potential measured at the reference field tensiometers. This setup ensured that the lysimeter simulated an "infinite" soil column. To assess the water balance, the lysimeters were positioned on three load cells (Model 3510, Tedea-Huntleigh, Canoga Park, CA, USA) that had a resolution of 1 g (equivalent to 0.001 mm precipitation and a water flux of 0.001 l). The leaching water extracted from 140 cm depth was collected and stored in water tanks that were positioned on a plateau balance with a resolution of 1 g (equivalent to a water flux of 0.001 l (Pütz et al. 2016). Data on load cells and plateau balance were stored every minute on the data logger.

Management history of soil, winter wheat cultivation, and ^{15}N labelled drip fertigation

The agricultural field, from which the soil monoliths were extracted, was utilized as grassland from 1961 to 1969. Subsequently, it was converted into a wheat field, and maize has been grown on the field since 1979. Immediately prior to the lysimeter extraction procedure in 2020, an oil radish cover crop was growing on the site. After the installation of the lysimeters at IMK-IFU, the soil was left fallow for one complete vegetative cycle to allow for the germination of residual seeds and weeds, followed by their removal. Campesino winter wheat (*Triticum sp.*), recommended for farmers in Bavarian regions (Bayerisches Staatsministerium für Ernährung 2021), was planted on the 28th of September 2020 in the lysimeters. We also grew winter wheat in the area surrounding the lysimeters (at least 5 m width) to protect the wheat plants inside the lysimeters from wind shear effects. Before planting, we performed manual tilling of the soil. The total wheat planting area was ca. 100 m^2 (including the wind shear protection zone around the lysimeters). In total, 171 kg N ha^{-1} mineral fertilizer NH_4NO_3 was applied: on the 20th of April (55 kg N ha^{-1}), the 1st (56 kg N ha^{-1}) and the 21st of June 2021 (60 kg N ha^{-1}). The sowing procedure, amounts of fertilizer and application intervals matched those used by conventional farmers. The ^{15}N enrichment was similar for NH_4^+-N and NO_3^--N and amounted to 71.66 atom% so as to determine recovery rates of the fertilizer N in various N pools (soil, plant biomass, roots, soil water, and gaseous emissions). The homogenous application of fertilizer in the lysimeters was achieved through a recently developed drip fertigation method (Tenspolde et al. 2023). To accomplish this, 219 bottles were used for fertigation of each lysimeter, with a water addition through the drip system of 22 l per lysimeter within a time span of 2 hours. During the 3rd fertilization, the wheat growth was dense and tall, which allowed for using only a reduced number of 102 bottles with extensions to pass the plants, equaling to application of 10.2 l through drip fertigation per lysimeter. Consequently, we added an additional 30 l of water in 5-liter pulses over 2 hours using a watering can. This approach was optimized to ensure the best possible 3-dimensional distribution of the ^{15}N tracer in the topsoil.

Sampling design

The timeline for sampling is presented in Fig. 2. Prior to the initial fertilizer application, soil samples were randomly collected from each lysimeter at sampling depths 0–5 cm and 5–30 cm. These samples were then homogenized and analyzed to determine the natural abundance isotopic enrichment of ^{15}N in total soil N. In addition to this, the natural abundance of ^{15}N in both aboveground biomass and

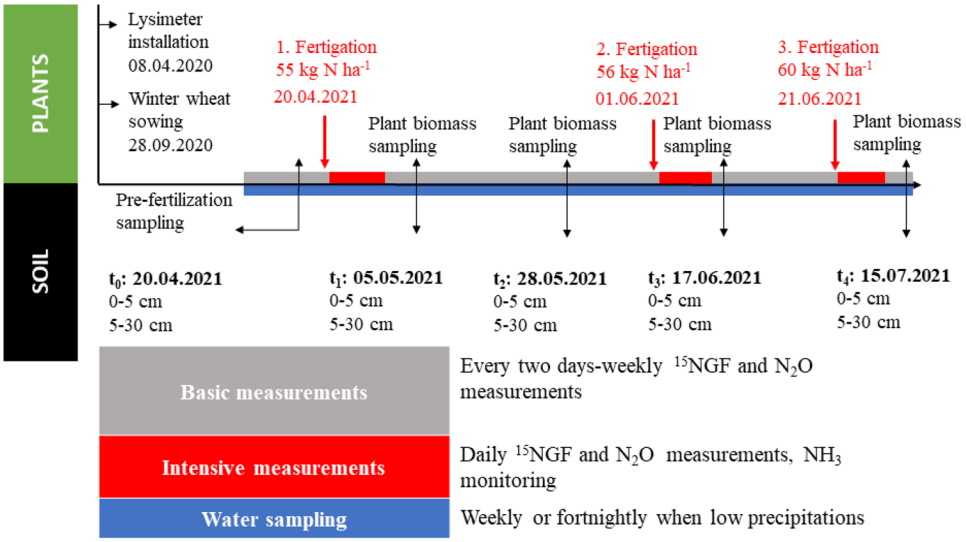

Fig. 2 The experimental timeline, including the sowing, fertilization, and sampling events for both soil and plant biomass. The frequency of different measurements is illustrated using grey, red, and blue colors. ^{15}NGF: ^{15}N gas flux method to measure N_2 emissions

roots of the plants growing on the lysimeters was also determined prior to fertilization. Following the application of ^{15}N labelled fertilizer, soil samples were collected from three replicates per lysimeter at depths of 0–5 cm and 5–30 cm, at four different time points (t1 to t4). For this, augers with inner diameters of 5 cm were used. On the same days of soil sampling, entire representative wheat plants, including roots, were harvested and analyzed ($N=1$ for the first three, $N=5$ for the final sampling). For the final sampling, motor-driven drilling equipment with plastic tube inliners (inner diameter 4.7 cm) was used to collect soil samples down to a depth of 1 m, as described by Zistl-Schlingmann et al. (2020). The five replicate soil cores per lysimeter were divided into depths of 0–30 cm, 30–60 cm, and 60–100 cm. Gravimetric soil water content was measured by drying freshly collected soil at each sampling time at 105 °C for 24 h.

Analytics

Measurement of N_2 emissions using the ^{15}NGF method

The ^{15}NGF method to quantify N_2 losses was applied daily in periods after fertilization, and on a weekly basis when the N_2 emissions had declined (Fig. 2). The chamber closure time varied between 120 and 270 min, depending on the chamber's height and proximity to the fertilization event. The static chambers, which covered the entire lysimeters (1 m^2), were equipped with a fan and initially had a height of 30 cm. As the wheat plants grew after the second fertilization, the chamber height was increased to 60 cm to prevent damage to the plants. Gas samples were collected (0 min, 60 min, and at the end of the closure time) using a syringe through a septum opening in the chamber and were subsequently inserted into a 12 ml pre-evacuated double septum exetainer (Labco Ltd. High Wycombe, UK) for analysis. Gas samples were analyzed for ^{15}N-N_2O and ^{15}N-N_2 using an Isoprime PrecisION isotope ratio mass spectrometer (Elementar UK Ltd. Stockport, UK), coupled to an iso FLOW GasBench (Elementar UK Ltd. Stockport, UK).

The calculation of N_2 and N_2O produced via denitrification was done using the ^{15}NGF method following the procedure described by Mulvaney (1984). Assuming that all of the N_2 and N_2O produced by denitrification come from the same pool of NO_3^-, the ^{15}N enrichment of the NO_3^- pool undergoing denitrification was derived from ^{15}N-N_2O. The ion currents (I) at m/z 44, 45, and 46 enabled the molecular ratios ^{45}R (^{45}I/^{44}I) and ^{46}R (^{46}I/^{44}I) to be calculated for N_2O. The ^{15}N enrichment of the NO_3^- pool undergoing denitrification (a_D) was then calculated from the non-random distribution of N_2O isotopologues using ^{45}R and ^{46}R as described by (Stevens and Laughlin 2001).

Fluxes of N_2 were calculated using a_D and the increase of ^{15}N-N_2 in the chamber headspace following denitrification. The ion currents at m/z 28, 29 and 30 enabled the molecular ratios ^{29}R (^{29}I/^{28}I) and ^{30}R (^{30}I/^{28}I) to be calculated for N_2. The differences between ambient and enriched atmospheres were expressed as Δ^{29}R and Δ^{30}R. The fraction of N_2 attributable to denitrification (d) in the chamber headspace was calculated according to Mulvaney and Kurtz (1984) using Δ^{30}R and the enrichment of the denitrifying pool a_D (Stevens and Laughlin 2001). Fluxes of N_2 were corrected for temperature and expressed on a surface basis in kg ha^{-1} day^{-1}. The fraction of fertilizer-derived N_2 (FD N_2) was calculated as the ratio of ^{15}N atom excess % of N_2 emitted and the ^{15}N atom excess % of the N fertilizer applied following the procedure described in Friedl et al. (2023).

The detection limit (DL) for N_2 emissions was determined by measuring $\Delta^{29}R$ and $\Delta^{30}R$ in atmospheric air samples using the method described in Friedl et al. (2020). The DL was calculated by multiplying the standard deviation (SD) of ambient air samples ($n = 17$) by the t-value at a confidence level of 95%. The SD for ^{29}R and ^{30}R of ambient air samples for each IRMS analysis, was 5.2448×10^{-6} and 1.6755×10^{-6}, respectively. The resulting DL values were 1.1067×10^{-5} for $\Delta^{29}R$ and 3.5354×10^{-6} for $\Delta^{30}R$. These DL values were used to set a lower limit of quantification for subsequent N_2 flux measurements, and fluxes below the DL were considered background fluxes. N_2 fluxes with negative $\Delta^{30}R$ values were discarded, corresponding to approximately 35% of the fluxes. The N_2 flux calculation, based on a_D, which showed a uniform distribution of ^{15}N after the fertilizer applications (Fig. S1), resulted in a detection limit of the method (MDL) of 0.003 g N m^{-2} day^{-1} (i.e., 0.03 kg N ha^{-1} day^{-1}) for a closure time of 3 h and chamber height of 0.3 m and 0.006 g N m^{-2} day^{-1} for a chamber height of 60 cm. If N_2 fluxes were below the DL, fluxes were set to 0.5 MDL following the procedure used by Friedl et al. (2023).

Linear interpolation was employed to estimate flux values for days when no measurements were conducted. During periods when the fluxes were not detectable, which typically occurred more than 2 weeks after fertilization events, the fluxes were assumed to be equal to 0.5 MDL for linear interpolation and cumulative flux calculation.

Measurement of other gaseous N losses

Ammonia losses were estimated using one cylindric manual chamber (150 mm diameter) per lysimeter. The chamber design is by Jantalia et al. (2012), and the underlying principle is NH_3 absorption in an acid trap. The chamber is formed of a rigid PVC cylinder that is 200 mm high. The open top is protected against rain with a roof 70 mm above the cylinder. Two polyurethane plastic foams (25 mm thick) acting as acid traps were soaked in 50 ml of a sulfuric acid solution (1 M H_2SO_4 and 4% (v/v) glycerol) and fixed in the chamber at 50 and 155 mm height above the soil surface. To facilitate the measurement of NH_3 emissions, three PVC frames (5 cm in height) were permanently installed on each lysimeter as a base for the ammonia chamber. Monitoring of NH_3 emissions occurred over a two-week period, commencing one day after each fertilization event. In the initial three days of measurement, the foam was replaced every 12 h. Subsequently, the foam switch frequency was adjusted to once a day for the following 7 days. Finally, the foams were changed every two days until the conclusion of the measurement period. For each NH_3 measurement, the chamber was set on a different basement to minimize chamber effects on soil and plants. At foam retrieval, the foam was vigorously compressed in a bag containing 150 ml of a 2 M potassium chloride (KCl) solution to extract the NH_4^+ cations and the foam extract was transferred into 50 ml falcon tubes and frozen for further analysis. The contents of NH_4^+-N in the extracts were measured using a colorimetric technique according to Kempers and Zweers (1986). The residual acid in the samples had to be neutralized, as the procedure requires alkaline conditions. We assumed that NH_4^+-N accumulations from the bottom foam equaled the NH_3-N emissions from the soil area covered by the chamber. ^{15}N enrichment could not be determined due to low NH_4^+ concentrations of the acid trap extract. We assumed that all NH_3 emissions were fertilizer-derived, which appears justified given that significant NH_3 emissions only occurred shortly after fertilization.

Nitrous oxide emissions were measured on a daily up to weekly basis, depending on the proximity to the fertilization events. For this, the large manual chambers covering the entire lysimeter that had been described earlier for N_2 emission measurements, were used. The chamber was connected to an Ultraportable Greenhouse Gas Analyzer (Los Gatos Research, San Jose, USA). The flux calculation relied on the N_2O concentration change inside the chamber as continuously measured over a period of 10–15 min, following the approach outlined by Ma et al. (2021a).

When the Greenhouse Gas Analyzer was unavailable, manual gas sampling from the chamber was conducted using a syringe, and the collected samples were placed into evacuated screw-cap Exetainers (12 ml), following the method described by Rehschuh et al. (2019). The chamber was then closed for a duration of 2 h. Subsequently, the samples were analyzed using a gas chromatograph connected to an autosampler (SRI 8610 C, SRI Instruments, Torrance, USA), as detailed in Rehschuh et al. (2019).

Soil air N_2O concentrations and $\delta^{15}N$ in N_2

To quantify soil air N_2O concentrations, we collected air samples from the semi-permeable membrane tubes (PP V8/2 HF membrane, Accurel®, Akzo Nobel Faser AG, Wuppertal, Germany), which were in equilibrium with soil air inside the lysimeters (Wolf et al. 2010), using a syringe, and then they were transferred into pre-evacuated screw-cap Exetainers (12 ml) through a septum (Wolf et al. 2010). The samples were subsequently analyzed by gas chromatography as described above. Using the same semi-permeable membrane tubes and sampling procedures, we also assessed ^{15}N enrichment in N_2 enrichment in the vertical soil air profile and analyzed the samples by Gasbench-IRMS as described above. To ensure the re-establishment of equilibrium with the soil air, we maintained a minimum time

interval of 6 h between subsequent sampling events of the membrane tubes. Sampling frequency for N_2O concentrations and $\delta^{15}N$ in N_2 ranged from daily after fertilization events to weekly in periods of background fluxes.

Inorganic N in soil water and N leaching

Mineral N in the soil solution was determined by collecting soil water samples from the bottles connected to suction cups (Fu et al. 2017). We collected water samples on a weekly basis or when sufficient water had accumulated in the bottles. The volume of water collected at each depth was determined, and a subsample of 50 ml was then filtered using a 0.45 µm hydrophilic cellulose acetate membrane (Sartorius Stedim Biotech GmbH, Göttingen, Germany) and a syringe. The filtered subsample was poured into Falcon tubes and stored in a frozen state until further analysis. Dissolved NH_4^+-N and NO_3^--N concentrations were determined colorimetrically using a microplate spectrometer (BioTek Instruments, Inc. USA) according to Kempers and Zweers (1986) and Pai et al. (2021). The amount of leached water was calculated based on the mass changes in the drainage tank of each lysimeter, while the threshold of 100 g min^{-1} was set to exclude occasionally observed outliers from the mass records. The amount of leached N was calculated by multiplying the cumulative water amount leached between two water sampling dates by the concentration of NH_4^+-N and NO_3^--N at 120 cm depth. In addition, subsamples were analyzed for $\delta^{15}N$ in NH_4^+-N and NO_3^--N using sequential diffusion (Wu et al. 2011).

Plant uptake and soil fates of fertilizer N

The aboveground (AGB) and belowground (BGB) biomass of the crop were calculated by multiplying the mean dry weight of wheat plant AGB/BGB ($N=3$ for the first two samplings, $N=15$ for the final sampling) by the lysimeter-specific number of plants counted at each sampling period. To analyze N concentrations and ^{15}N enrichment in plant, root and soil, samples were dried at 60 °C according to Zistl-Schlingmann et al. (2020). The dry soil and plant samples were then ground using a pebble mill and subsequently packed into tin capsules. The concentration and isotope ratio of N was determined using an elemental analyzer (Flash EA, Thermo Scientific, Waltham, MA, USA) coupled to an isotope ratio mass spectrometer (Delta PlusXP, Thermo Scientific, Waltham, MA, USA) as described in detail by Zistl-Schlingmann et al. (2020).

The excess ^{15}N amount in plant and soil pools was calculated using the following equation:

$$N_{pool} \times \left(\frac{APE}{100}\right) (1)$$

where N_{pool} is the amount of N in mg, found in the soil or plant pool and APE (atomic percent excess) is the ^{15}N excess enrichment of the respective pool. APE is determined by subtracting the natural abundance ^{15}N enrichment (atom% ^{15}N) from the measured value of atom% ^{15}N of the associated N pool.

Recovery of the fertilizer N in investigated N pools was calculated by dividing the ^{15}N excess amount of the respective N pool by the cumulative amount of fertilizer ^{15}N excess added to the lysimeters at the corresponding sampling time. For scaling of soil ^{15}N recovery to the lysimeter level, sampling depth, volume and bulk density were considered (Zistl-Schlingmann et al. 2020). We then multiplied ^{15}N excess recovery (% of added ^{15}N excess) by fertilizer N addition rate (kg N ha^{-1}) to obtain the flow of fertilizer-N into the investigated N pools. More detailed calculation procedures for the ^{15}N tracing approach into plant and soil N pools are provided by Dannenmann et al. (2016, supplementary material).

Fertilizer N balance

The cumulative emissions of N_2, N_2O, and NH_3 were calculated for single sampling dates, and over the entire duration of the study. To account for days when no measurements of NH_3, N_2O, and N_2 were taken, a linear interpolation was applied (see above for details on N_2 interpolation). The "unaccounted fertilizer N" – which may be interpreted as N_2 emissions - was calculated by subtracting the fertilizer N flows into soil N, plant N, leaching water N, and gaseous emissions (excluding N_2) from fertilizer N addition. These fertilizer N balances were set up separately for all four sampling dates where plant, soil and ^{15}NGF data were available.

Statistical analysis

The statistical analyses were conducted using the open-source programming language Python (version 3.6.0, Python Software Foundation) and R version 4.2.0 (R Core Team 2019). The graphs were made using Origin, version 2020b (OriginLab Corporation 2020). The three lysimeters were used as replications in the experiment, making the lysimeter the statistical unit. The five replicated soil cores or plants obtained during each harvest were treated as pseudoreplicates. Mean values and standard error of the mean were calculated using $N=3$ lysimeters. To assess the statistical difference between the results obtained with the ^{15}NGF method and the ^{15}N mass balance approach, the Wilcoxon Signed Ranks Test was used.

Results

N_2, N_2O and NH_3 emissions, and soil water nitrate

The emissions of N_2 (Fig. 3a) showed large variations across the three instances of fertilization. Largest N_2 fluxes were observed with delays ranging from a few days to 3 weeks after the first fertilization event (April 21st), with a maximum flux of > 3 kg N ha^{-1} day^{-1} on May 8. These delayed N_2 emission peaks occurred with warming soil (Fig. 3g), and in particular, after precipitation events that increased WFPS in topsoil (Fig. 3f). It should also be noted that these high N_2 emission peaks were observed at a time when plant N acquisition, with cumulative uptake of 14 ± 2 kg N ha^{-1}, was still relatively low (Table 1a). In addition to the increased topsoil NO_3^- concentrations originating from the ^{15}N-labelled fertilizer, we also observed high NO_3^- concentrations at depths greater than 50 cm (Fig. 3e). High subsoil NO_3^- concentrations originated from downward movement of NO_3^- during the preceding winter (data not shown), which finally reached depths of > 100 cm at the end of the growing season. This was also confirmed by only insignificant ^{15}N enrichment in leached NO_3^- at 120 cm depth, while NH_4^+ was at the detection limit in the leachate. The total amount of leached NO_3^- during the measurement period accounted for 3.1 ± 0.3 kg N ha^{-1} (detailed monthly water and NO_3^- leaching data are provided in Table S1). However, the leaching of recent fertilizer N during the monitored period was with only 0.04 ± 0.02 kg N ha^{-1} very small (Table 1a).

Unlike the emissions observed after the first fertilization, the N_2 emissions following the 2nd fertilization exhibited a brief peak-like response, remained smaller than 0.42 kg N ha^{-1} day^{-1} and returned to background levels within 6 days (Fig. 3a). The increase in N_2 emissions was observed already within 2–3 h after fertilizer application. Dinitrogen emissions were lowest after the 3rd fertilization, despite higher soil temperatures compared to earlier fertilization events (Fig. 3a, g). These lower N_2 peak emissions after the 2nd and 3rd fertilization corresponded to periods of large plant N uptake, i.e., up to half of fertilizer N was recovered in plant biomass (Table 1a, b).

The total cumulative N_2 losses at the end of the experiment were 21 ± 3 kg N ha^{-1} (Table 1a). Among these losses, the N_2 losses derived from the fertilizer accounted for 13 ± 2 kg N ha^{-1}, equivalent to 7.5 ± 0.9% (Table 1a, b) of the applied fertilizer.

The N_2O flux pattern after the first fertilization in April equaled that of N_2 emissions, i.e., showed sporadic emissions over ca. three weeks with occasionally high variability across lysimeters. Following the 2nd fertilization, N_2O emissions exhibited a sharp peak response, with the highest emissions observed one day after fertilization amounting to 0.008 ± 0.002 kg N ha^{-1} day^{-1}. Following the peak emission, the N_2O emissions quickly decreased and returned to background levels in the subsequent days. After the 3rd fertilization on June 21, N_2O emissions were of similar magnitude compared to the second fertilization, but lasted longer. Throughout the measurement period of 2.5 months, a total of 0.15 ± 0.01 kg N_2O-N ha^{-1} was emitted. Given the small N_2O emissions in contrast to the significant N_2 emissions the resulting N_2:($N_2O + N_2$) ratio was on average 0.94 ± 0.06, with a maximum of 1.001 and a minimum of 0.75.

After the first fertilization event, NH_3 emissions peaked at 0.228 ± 0.006 kg N ha^{-1} day^{-1} on day 5 and then rapidly declined, becoming undetectable until the next fertilization event (Fig. 4). After subsequent fertilization events, similar patterns of NH_3 emissions were observed. Following the 2nd fertilization event, peak emissions reached only 0.04 kg N ha^{-1} day^{-1}, while after the 3rd fertilization, emissions peaked at 0.15 ± 0.01 kg N ha^{-1} day^{-1} on days 1 and 2 following fertilization, before gradually declining within 7 days to values below the detection limit. The cumulative emissions of NH_3 after the first fertilization event were 1.1 ± 0.1 kg N ha^{-1}, while the total cumulative emissions for the entire intensive measurement period were 1.5 ± 0.1 kg N ha^{-1} or 0.87 ± 0.03% of the applied fertilizer (Table 1a, b). Hence, both NH_3 and N_2 emissions mainly occurred after the first fertilization, but were of lower importance later in the growing season, when temperature was higher, but large proportions of fertilizer N were allocated to plants.

Fertilizer N mass balance and comparison of unaccounted fertilizer N fates with directly measured N_2emissions

Across all four sampling dates, between 32% and 64% (equivalent to 21–78 kg N ha^{-1}) of the applied fertilizer N was recovered in the soil, making it the primary sink for the fertilizer N (Table 1a, b). Plant uptake was of equal importance, with 26–52% (14–73 kg N ha^{-1}) of the added fertilizer N being taken up by the plants at the respective sampling dates (Table 1a, b). In contrast, cumulative NH_3 losses were only 1.5 kg N ha^{-1} over the entire period (less than 1% of added fertilizer N), which still was much larger than the cumulative N_2O emissions, which only accounted for 0.1% of added fertilizer N. Leaching of fertilizer N was even lower compared to N_2O emissions, and thus negligible for the fertilizer mass balance.

Based on these fertilizer N fates, 8–33% of fertilizer N remained unaccounted across the sampling dates (Table 1b). This translates to an unaccounted fertilizer N loss that increased from 4 ± 2 to 18 ± 13 kg N ha^{-1} over time (Table 1a). Parallel direct measurements of N_2 losses using the ^{15}NGF method revealed fertilizer N_2 losses of

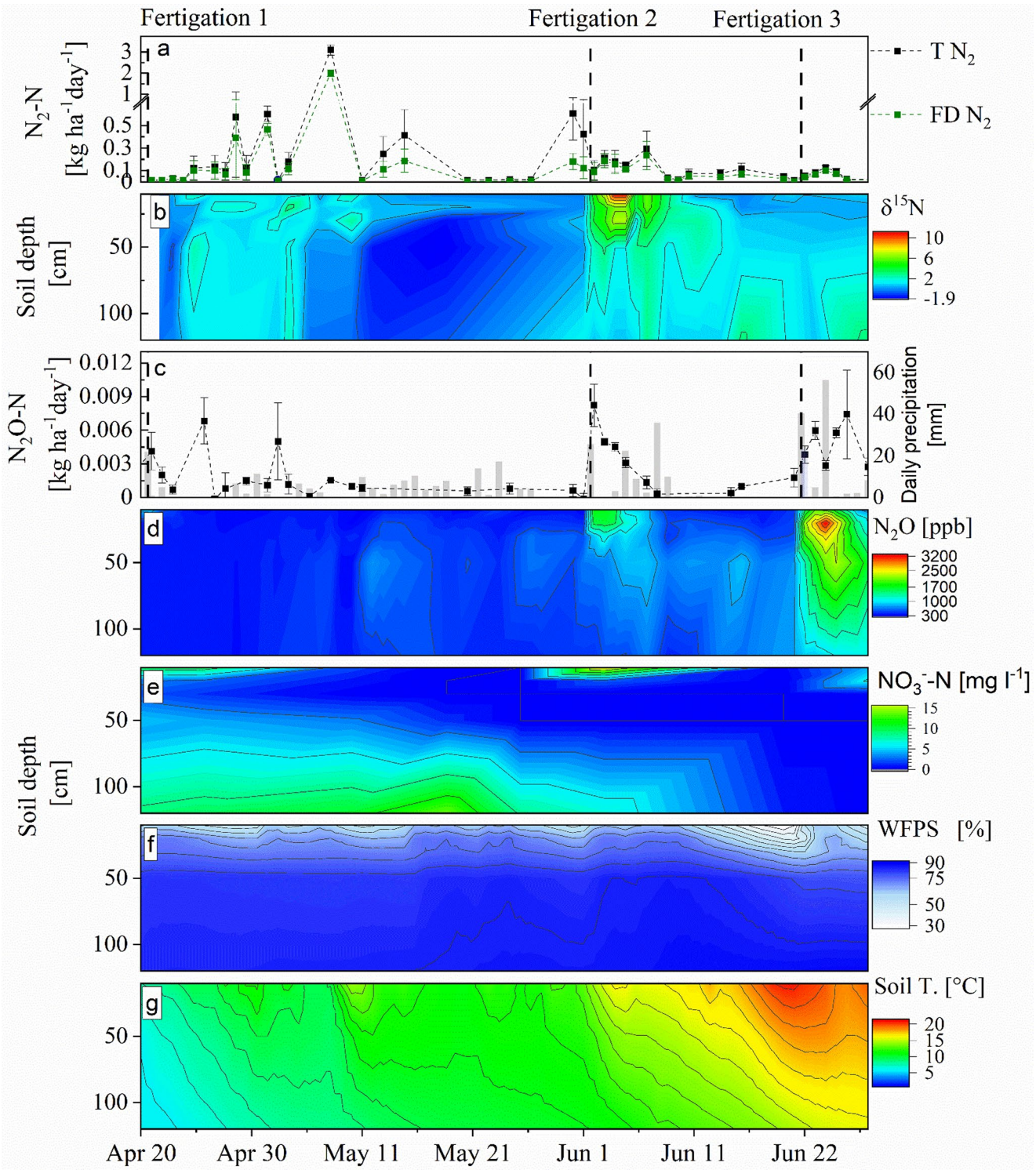

Fig. 3 Soil N_2 emissions as measured by the ^{15}NGF method from the entire 1 m^2 lysimeter areas ($N=3$). The black symbols represent the total N_2 soil emissions (T N_2), the green symbols represent fertilizer N derived N_2 flux (FD N_2) (**a**); ^{15}N enrichment profile of soil air N_2 (**b**); Total soil N_2O emissions measured from the entire lysimeter area and daily precipitation (including drip fertigation) (**c**); soil air N_2O concentrations profile (**d**), soil water NO_3^--N concentrations profile in mg N l^{-1} (**e**); soil water-filled pore space profile, in % (**f**); soil temperature profile, in °C (**g**). All values provided are mean values of the 3 analyzed lysimeters. The error bars for fluxes indicate SE. Fertigation events are visually represented in the flux graphs by vertical dashed lines

Table 1(a) Fertilizer N balances for the different sampling times (t1 to t4), as calculated from respective ^{15}N recovery rates (Table 1b). The table shows N inputs by fertilizer addition, as well as fertilizer N fates, soil storage, plant uptake (including roots), N leaching, as well as N_2O and NH_3 emissions. This information then is used to calculate the unaccounted fate of fertilizer N, which should equal fertilizer-derived N_2 emissions. The last two lines then provide the directly measured cumulative N_2 emissions by use of the ^{15}NGF method, separately for fertilizer-derived emissions and total emissions. Uncertainty is provided as the standard error of the mean of $N = 3$ lysimeters

N pool (kg N ha^{-1})	t_1 5/5/2021	t_2 28/5/2021	t_3 17/6/2021	t_4 15/7/2021
Fertilizer addition	55	55	111	171
Fertilizer N in soil	35 ± 2	21 ± 5	36 ± 2	78 ± 9
Fertilizer N uptake by plants (incl. roots)	14 ± 2	14 ± 5	57 ± 9	73 ± 6
Leaching of fertilizer N	0.02 ± 0.01	0.04 ± 0.02	0.04 ± 0.02	0.04 ± 0.02
Total N_2O emissions	0.037 ± 0.005	0.055 ± 0.003	0.086 ± 0.003	0.15 ± 0.01
Total NH_3 emissions	1.1 ± 0.1	1.2 ± 0.1	1.3 ± 0.1	1.5 ± 0.1
Unaccounted fertilizer N fates (mass balance)	**4 ± 2**	**18 ± 9**	**17 ± 9**	**18 ± 13**
Measured cumulative fertilizer N_2 losses	**2.4 ± 0.5**	**10 ± 1**	**12 ± 2**	**13 ± 2**
Measured total N_2 losses	3.3 ± 0.7	16 ± 2	20 ± 3	21 ± 3

Note: No statistically significant differences were observed between unaccounted fertilizer N loss of the mass balance and corresponding directly measured N_2 emissions

The bold format was used to highlight the main outcome for this table

Table 1(b) Fertilizer N fates expressed in % of fertilizer applied until the respective sampling dates (t1-t4). Error bars represent the standard error of the mean. The percentage of unrecovered fertilizer N loss was not statistically different compared to directly measured fertilizer-derived N_2 emissions, expressed in % of applied fertilizer. Note that t1 and t2 samplings were after the first ^{15}N application, t3 after already two, and t4 after all three ^{15}N applications. This explains e.g., the increase of fertilizer N recovery in soil between t3 and t4

Fertilizer N recovery (%)	t_1 5/5/2021	t_2 28/5/2021	t_3 17/6/2021	t_4 15/7/2021
Fertilizer N in soil	64 ± 3	39 ± 9	32 ± 2	46 ± 5
Fertilizer N uptake by plants (incl. roots)	26 ± 4	26 ± 9	52 ± 8	43 ± 4
Leaching of fertilizer N	0.04 ± 0.02	0.07 ± 0.04	0.04 ± 0.02	0.02 ± 0.01
N_2O emissions	0.07 ± 0.01	0.10 ± 0.01	0.077 ± 0.003	0.09 ± 0.01
NH_3 emissions	2.0 ± 0.2	2.2 ± 0.2	1.1 ± 0.1	0.87 ± 0.03
Unaccounted fertilizer N fates	**8 ± 4**	**33 ± 17**	**15 ± 9**	**11 ± 8**
Measured cumulative fertilizer N_2 losses, expressed in % of applied fertilizer N	**4.4 ± 0.9**	**18.5 ± 1.6**	**11.1 ± 1.4**	**7.5 ± 0.9**

Note: No statistically significant differences were observed between unaccounted fertilizer N loss of the mass balance and corresponding directly measured N_2 emissions

The bold format was used to highlight the main outcome for this table

2.4 ± 0.5 kg N ha^{-1} that increased to 13 ± 2 kg N ha^{-1} and total N_2 losses that increased from 3.3 ± 0.7 kg N ha^{-1} to 21 ± 3 kg N ha^{-1}. Both directly measured fertilizer N_2 emissions and total N_2 emissions were not statistically different compared to unaccounted fertilizer N loss of the mass balance approach. Directly measured cumulative fertilizer N_2 emissions increased in particular between May 5 and May 28, i.e., from 2.4 ± 0.5 to 10 ± 1 kg N ha^{-1}, with little increase in the remaining experimental period (Table 1a). Also, this was in excellent agreement with the findings of the fertilizer mass balance approach, which during the same time indicated an increase in N_2 emissions (via unrecovered fertilizer ^{15}N) from 4 ± 2 to 18 ± 9 kg N ha^{-1}. Hence, the mass balance approach did not only represent directly measured cumulative N_2 emissions at the end of the measuring period, but also identified the highest N_2 emissions in the same time span as observed by the ^{15}NGF measurements.

While N_2 and N_2O emissions represent fluxes between the soil and the atmosphere for 1 m^2 area of the lysimeters, vertical soil information on ^{15}N enrichment in N_2 and on N_2O concentration was obtained from the installed semi-permeable membrane tubes that reflect a smaller fraction of the lysimeters soil air (Fig. 3b and d). Nonetheless, the patterns of $\delta^{15}N_2$ in lysimeter soil air generally reflected the temporal dynamics of measured N_2 emissions. Specifically, this included the delayed response and the extended overall length of N_2 emission after the first fertilization. Unfortunately, on the day of the highest N_2 emissions beginning of May, we did not measure corresponding soil profile data of $\delta^{15}N_2$. This is because the sampling frequency had declined as we did not expect high emissions to occur weeks after the fertilization event. After the 2nd fertilization, peak N_2 fluxes were accompanied by clear increases of $\delta^{15}N_2$ values in the soil air right over the duration of the N_2 emissions

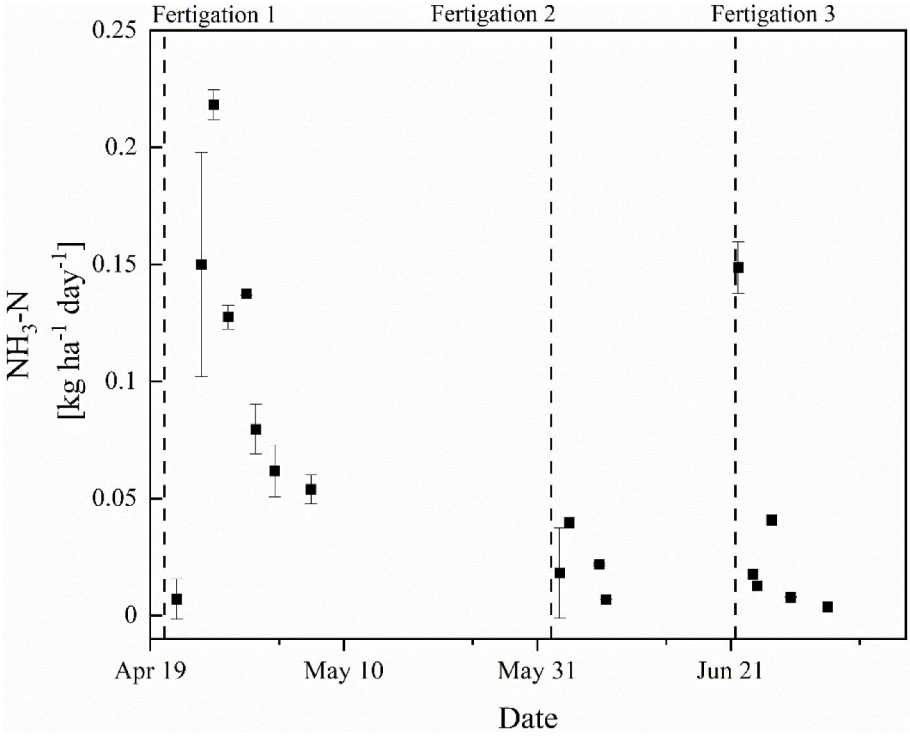

Fig. 4 Ammonia emissions in kg N ha^{-1} day^{-1} after each fertigation event. The fertigation events are represented by dashed lines. The error bars indicate the standard error (SE) of the mean

peak. Finally, the only very low N_2 emissions after the 3rd fertilization were also hardly visible in form of $\delta^{15}N_2$ increases in the topsoil. However, it needs to be noted that the highest soil air $\delta^{15}N_2$ values did not necessarily correspond to the highest N_2 emissions at the soil-atmosphere interface. This was also reflected by the results of a regression analysis, which on the one hand indicated a significant positive relationship between N_2 flux and $\delta^{15}N$ in soil air at 10–50 cm depths ($p < 0.01$) (Fig. 5a). On the other hand, the regression model only explained up to 52% of the variability observed in N_2 emissions across the measurements, with a further strongly decreasing explanatory power at greater depths. Very similar results were obtained for the relationships between soil air N_2O concentrations and N_2O emissions at the soil-atmosphere interface (Figs. 3c and d and 5b). The dynamics of soil air N_2O concentrations generally corresponded to the peaks in N_2O emissions following the 2nd and 3rd fertilization events, while the magnitude of N_2O concentrations varied significantly despite comparable emissions. Additionally, the sporadic N_2O emissions observed after the first fertilization event did not result in commensurate increases in soil air N_2O concentrations. The results of regression analysis indicated a strong correlation between the N_2O flux and N_2O concentration in three depths- 10, 20 and 30 cm ($p = 0.000$, $p = 0.01$, $p = 0.013$, respectively), while the R^2 at 10 cm depth was the highest and decreased with depth, similar to the pattern observed for N_2 emissions vs. $\delta^{15}N_2$ in soil air ($R^2 = 0.48$, $R^2 = 0.32$ and $R^2 = 0.21$, respectively) (Fig. 5b).

Discussion

The role of N_2 emissions in the fertilizer N balance of fertigated winter wheat

Total N_2 emissions (including those not from applied fertilizer) in our study were the dominating N loss and exceeded NH_3 emissions by approximately one order of magnitude, and N_2O emissions by two orders of magnitude, while overall fertilizer N losses remained low with about 12% of applied fertilizer compared to plant uptake and soil storage (Table 1).

Denitrification losses from agricultural soils and its product stoichiometry, as well as NH_3 emissions are governed by climate and soil properties, but to a large extent also by management, which might be of particular importance in our study as the fertilization was done in conjunction with irrigation, i.e., by fertigation. Total NH_3 emissions in our study were about 1% of applied fertilizer N and, thus, much smaller than the global NH_3 emission factor for the use of synthetic fertilizer N (12.56%), the NH_3 emission factor for use of synthetic N in Europe (6%) or the global NH_3 emission factor for wheat cultivation (12.05%) (Ma et al. 2021b). Nitrous oxide emissions measured during our monitoring period accounted for only ca. 0.1% of fertilizer N, which is also low compared to the German national emission factor for direct N_2O emissions from synthetic fertilizers, which is 0.6% (Mathivanan et al. 2021).

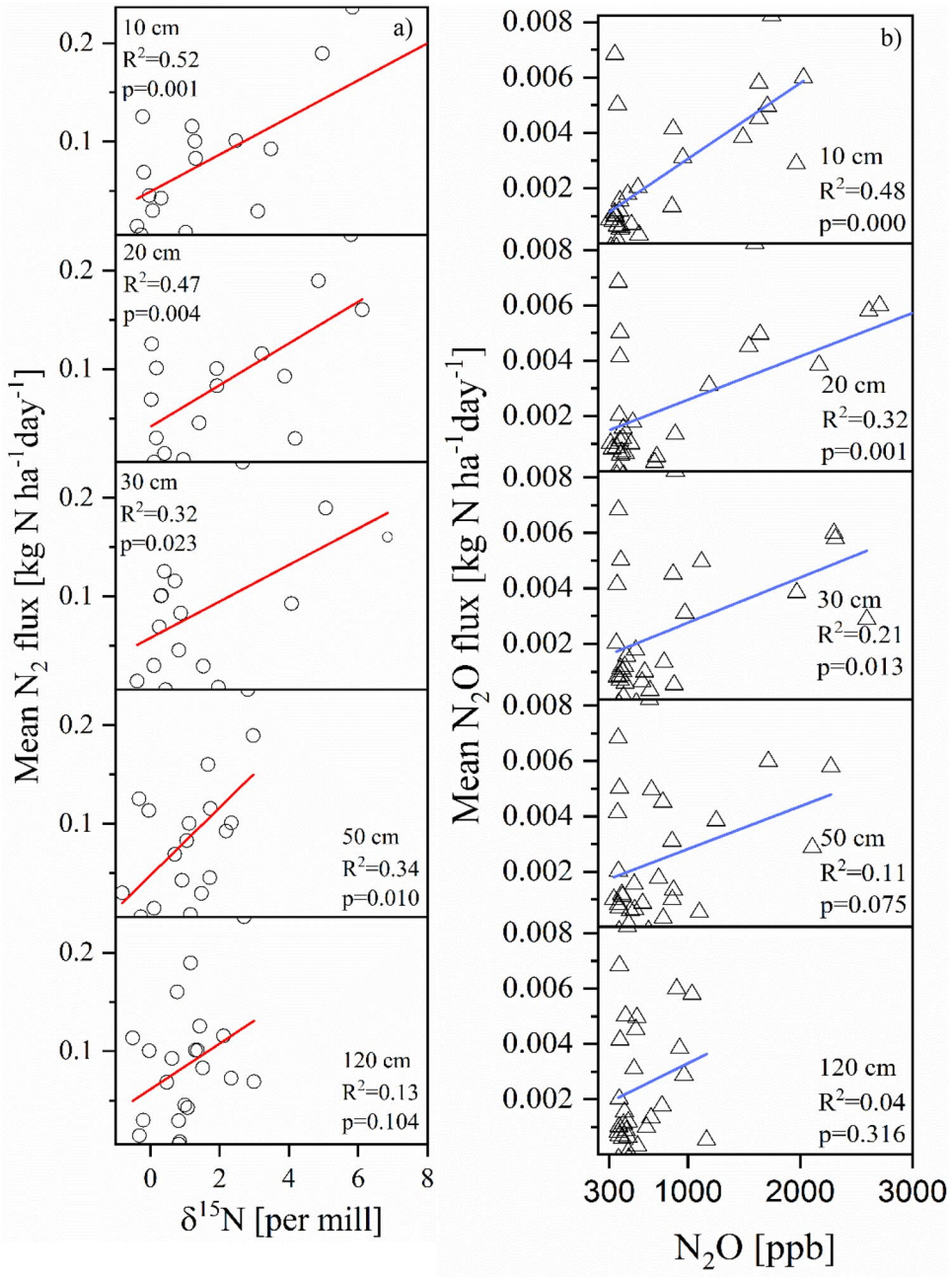

Fig. 5 (**a**) Regression analysis of the mean fertilizer-derived N_2 flux and $\delta^{15}N_2$ values for various depths (10 cm, 20 cm, 30 cm, 50 cm, and 120 cm), only when were measured at the same day; (**b**) Regression analysis of the mean total N_2O flux and N_2O concentrations in ppb in all the depths. Each data point represents the average value for a specific depth and time point. The fluxes are in kg N ha^{-1} day^{-1}. The solid lines represent linear regression lines fitted to the data. The p-values provide statistical significance of the relationships

In contrast to NH_3 and N_2O emissions, much less is known on fertilizer-induced N_2 emissions. Recently, Pan et al. (2022b) provided estimates of emission factors of denitrification (N_2+N_2O) based on a global synthesis and obtained a global mean value of 4.7% of applied fertilizer. However, the dataset in this study is strongly dominated by AIT studies so that this emission factor might be underestimated. The total N_2 losses in this study were found to be 21 ± 3 kg N ha^{-1} in 2.5 months (or fertilizer-derived N_2 losses of 13 ± 2 kg N ha^{-1} $season^{-1}$, i.e., 7.5 ± 0.9% of fertilizer N input). These values are comparable to the results of Rolston et al. (1978), who used the ^{15}NGF method to evaluate field N_2 fluxes in summer-period (23 °C) cropped plots (perennial ryegrass) in Typic Xerorthent, fertilized with enriched KNO_3 under two water regimes close to saturation. In the latter study, the cumulative N_2 flux was 7–30 kg N ha^{-1} accounting for 3–14% of the fertilizer N. Mosier et al. (1986b), measured N_2 fluxes from barley and corn miniplots in Nunn clay loam during the summer season in Colorado. They used the ^{15}NGF method to assess N_2 seasonal emissions of 1.5 and 0.7 kg N ha^{-1} for corn and barley, respectively, after the application of enriched $(NH_4)_2SO_4$. These emissions accounted for only around 1–2% of the applied N, possibly because of high N use efficiency of the crop.

Recent studies conducted in Germany, on Haplic Luvisol crop systems using cattle slurry organic fertilizer and enriched $K^{15}NO_3$, reported N_2 emissions of 0.4 to 3 kg N ha^{-1} or 0.6–3.9% of the total N input (Buchen-Tschiskale et al. 2023). The study's findings of minor $N_2 + N_2O$ losses but high NH_3 emissions of up to 8 kg N ha^{-1} are typical for the application of liquid cattle slurry fertilizer. In a study conducted by Pan et al. (2022a) in northeastern China, characterized by a cool temperate, sub-humid continental monsoon climate and cultivated black soil, similarly low N_2 emissions of 1.6 ± 0.5 kg N_2-N ha^{-1} were reported, accounting for only 0.7% of the applied $(^{15}NH_4)_2SO_4$-N input. In the latter case, with measurements in the spring season, low temperatures might explain the N_2 emissions. Vice versa, N_2 emissions can be particularly high in tropical regions. For instance, Takeda et al. (2023) investigated denitrification emissions in intensively managed tropical sugarcane farms, revealing exponentially increasing denitrification losses (ranging from 12 to 87 kg N ha^{-1} $season^{-1}$) with increasing N fertilizer rates from 0 to 250 kg N ha^{-1}. These emissions accounted for as much as 31–78% of the mineral fertilizer ^{15}N losses, with the primary component being N_2.

We attribute the fertilizer N fate patterns of our study, characterized by high plant N uptake and soil storage along with low overall gaseous N losses that are dominated by N_2 emissions rather than NH_3 emissions, to the drip fertigation management. While our primary motivation for using drip fertigation was to achieve homogenous ^{15}N labelling, decreased leaching and reduced NH_3 emissions, our findings indicate a range of beneficial effects of drip fertigation in the temperate climate conditions of this study where its application is not common. However, a control with normal fertilization was not included in this study. Recent research confirmed that drip fertigation does not only strongly increase water use efficiency, but also N use efficiency (Anas et al. 2020). It reduces NH_3 and N_2O emissions and NO_3^- leaching (Zheng et al. 2023), but possibly increases the relative importance of denitrification over NH_3 emissions (Qasim et al. 2022). A significant and unresolved question in this context is the extent to which N_2O losses are mitigated by complete denitrification until the terminal product N_2. In our study, with a pH value of 6.7, high WFPS and low soil NO_3^-, there were several factors that promote denitrification until the terminal product N_2 and thus might explain the large importance of N_2 emissions over N_2O emissions (Butterbach-Bahl et al. 2013).

Comparison of unrecovered fertilizer N with directly measured N_2 emissions to verify field ^{15}NGF measurements

Fertilizer-derived N_2 emissions as obtained from the ^{15}NGF method are subject to method-inherent bias that is difficult to constrain, e.g., underestimation of N_2 losses due to heterogeneous tracer application and $^{15}N_2$ subsoil diffusion and storage (Arah 1992; Friedl et al. 2020; Micucci et al. 2023; Vanden Heuvel et al. 1988). Also, the ^{15}N fertilizer mass balance approach is subject to uncertainty, given the many components of the N mass balance that need to be considered such as uncertainty in quantifying above and belowground biomass N or N compounds along the soil profile.

In this context, the most striking finding of this study was that directly measured fertilizer-derived N_2 emissions were statistically similar to the unaccounted fertilizer N fates of the ^{15}N fertilizer mass balance approach for all four sampling dates conducted during three fertigation events. Still, the total cumulative fertilizer-derived N_2 emissions persistently showed smaller numbers (by 28–44%) than the gap in the ^{15}N fertilizer mass balance. It could be argued that this discrepancy might be attributed to the aforementioned issues of the ^{15}NGF method, leading to an underestimation of N_2 formation. However, this remains generally speculative, given the remaining uncertainties of the fertilizer N mass balance approach.

The experimental design of this study was optimized in several regards to facilitate this method comparison. In our study, only NO emissions and DON leaching were not accounted for in the ^{15}N mass balance, which however are expected to be negligible (a) given the high N_2:N_2O ratios and very low N_2O emissions, which suggest a small role of NO as well (Butterbach-Bahl et al. 2013) and (b) the very low NO_3^- leaching losses in our study. Consequently, we were able to reduce uncertainty in ^{15}N fertilizer mass balance, largely attributed to its fates in plants and soil, which significantly improved the overall accuracy of the approach. Despite this, the uncertainty in constraining unrecovered ^{15}N based on lysimeter triplication remained larger compared to that obtained for direct N_2 measurements using the ^{15}NGF method. Furthermore, the slow drip fertigation application method did not only maximize the homogeneity of ^{15}N application (Tenspolde et al. 2023) and thus, the representativeness of soil sampling, but likely reduced NH_3 emissions and their role in the fertilizer N mass balance. The latter, together with the low NO_3^- leaching from fertilizer strongly reduced the accumulation of uncertainty in the ^{15}N fertilizer mass balance. Such uncertainty often prevents the setup of an accurate ^{15}N fertilizer budget under field conditions (Micucci et al. 2023; Myrold 1990).

To enhance the accuracy of ^{15}NGF measurements, we employed closed lysimeter systems, that might limit underestimation of N_2 emissions due to ^{15}N subsoil diffusion (Friedl et al. 2020; Well et al. 2019b). This underestimation may be in the order of magnitude of 1/3 or more (Micucci et al. 2023) and might possibly be smaller in our approach as ^{15}N enriched gases could not leave the closed bottom of the lysimeters. Additionally, as we set up our experiments in lysimeters we avoided typical weaknesses associated with the ^{15}N fertilizer mass balance approach such as unclear spatial boundaries (Micucci et al. 2023), and difficult quantification of N leaching losses. To further optimize the accuracy of the ^{15}NGF method, we applied high ^{15}N fertilizer enrichment with optimized homogeneity (Tenspolde et al. 2023). We minimized the chamber height according to the current crop height to enhance the detection limit of the ^{15}NGF method during the early stages of plant growth (Friedl et al. 2020; Micucci et al. 2023). In our study, the N_2 flux detection limit varied based on chamber height (30 to 60 cm) between 0.003 g N m^{-2} day^{-1} for 30 cm height and 0.006 g N m^{-2} day^{-1} for 60 cm chamber height. Recently, Liu et al. (2022) reported similar detection limits for in situ ^{15}NGF method application in maize and wheat fields, which was as low as 0.001–0.006 g N m^{-2} day^{-1} for six hours of chamber closure, while for two hours the detection limit was 0.004–0.037 g N m^{-2} day^{-1}. It is worth noting that the chamber used had a height of 3 cm in that study, which prevented the inclusion of plants within the chamber. Similar ranges of detection limits were reported in other studies (0.003–0.022 g N m^{-2} day^{-1}), however, they all used lower chamber heights (Bergsma et al. 2001; Buchen et al. 2016; Tauchnitz et al. 2015).

In our study, the static chambers used to directly measure N_2 emissions extended to the entire lysimeter area of 3 m^2. This approach was chosen to prevent the risk of overlooking small-scale denitrification hot spots (see e.g., Parkin 1987). In contrast to spatial resolution, we attribute significant uncertainty of direct N_2 emission measurements in our study to the restricted temporal resolution, which leads to uncertainties during interpolation and cumulation of N_2 emissions. This may explain the relatively low cumulative fertilizer-derived N_2 emissions compared to the mass balance approach between May 5th and May 28th (Table 1a), i.e., further sporadic N_2 emission peaks were probably missed. On the other hand, the highest directly measured N_2 emissions measurements between t1 and t2 were accompanied by a concomitant increase in unrecovered fertilizer N in that period, again demonstrating that results of the ^{15}NGF method aligned well with the ^{15}N fertilizer mass balance approach. Considering the low plant N uptake in this period (Table 1a), the relatively high N_2 emissions were likely facilitated by low competition by plants, while fertilizer-induced increases in topsoil NO_3^- concentrations were already diminishing (Fig. 3e).

Similar to our work, Rolston et al. (1979) compared the ^{15}NGF method to quantify N_2 emissions with a fertilizer mass balance approach under field conditions. This study reported direct measurements of total denitrification to be generally much smaller compared to estimates obtained from the mass balance approach (up to 65 kg N ha^{-1}). The difficulties to compare the two approaches were assigned to both methods – the large detection limit of the ^{15}NGF method to quantify N_2 (0.1 g N $m^{-2}day^{-1}$), the limited temporal resolution of direct flux measurements, and huge uncertainties in the quantification of the different ^{15}N fertilizer fates such as leaching and soil storage. Recently, Buchen-Tschiskale et al. (2023) compared directly measured N_2 emissions from the ^{15}NGF method under reduced ambient N_2 atmosphere with a ^{15}N mass balance approach using organic slurry fertilizer applied to winter wheat. This study revealed that for certain slurry application treatments, $N_2 + N_2O$ losses matched well with the ^{15}N recovery, while for others, they did not, with the large NH_3 emissions possibly being the dominating source of uncertainty. These earlier studies thus illustrate that it was essential that in this study the uncertainty of both methods could be reduced.

Kulkarni (2014) compared the ^{15}NGF method with the He gas-flow soil core method under laboratory conditions using unfertilized forest soils. This comparison did not reveal comparable or related rates of N_2 loss, which was likely related to the use of different soil samples and addition of N amounts to unfertilized soil only in the ^{15}NGF method. Generally, the application of the ^{15}NGF method to unfertilized forest soils appears questionable due to the need to add large $^{15}NO_3^-$ amounts which will perturbate denitrification processes (Friedl et al. 2020). Furthermore, the He gas-flow soil core method reveals total N_2 emissions, irrespective of source processes, fertilizer-N and other sources, and from all origins along the entire vertical soil profile. In contrast, the ^{15}NGF method only reveals total N_2 emissions from NO_3^- pools that were well mixed with ^{15}N-enriched NO_3^-, i.e., do not include emissions from unlabeled NO_3^- in subsoil. Given the significant subsoil NO_3^- concentrations, accompanied by persistently high WFPS (Fig. 3), we might indeed have underestimated total N_2 emissions in this study. This however does not affect our comparison between fertilizer-derived N_2 emissions and unaccounted ^{15}N of the ^{15}N fertilizer mass balance.

In conclusion, due to our targeted lysimeter setup, we were able to reduce the uncertainty of the ^{15}N fertilizer mass balance to an extent that allowed for a direct comparison with directly measured N_2 losses obtained from the ^{15}NGF method. This provided independent confirmation of

the ^{15}NGF measurements under ambient atmospheric conditions for multiple soil and plant sampling dates.

Relationships between measured N emissions and soil air measurements

In our second hypothesis, we expected a link between changes in ^{15}N enrichment of N_2 in the soil profile and measured N_2 fluxes at the soil-atmosphere interface. This was partly confirmed due to the general but not universal relationships between variations in δ^{15}N enrichment of N_2 in the soil profile and measured N_2 emissions at the soil-atmosphere interface (Fig. 5a), which were also reflected in significant correlations. Analogously to N_2 emissions, a positive correlation of N_2O emissions with N_2O concentrations in the soil at 10–30 cm depth was found. These similarities in the relationships between soil air data and fluxes observed for N_2O and N_2 emissions indicate the presence of a relationship between soil air of $\delta^{15}N_2$ and N_2O concentrations to associated fluxes at the soil atmosphere interface.

To our knowledge, no comparable study is available on soil air δ^{15}N dynamics. However, our N_2O-related findings align well with the results of Li et al. (2021), who demonstrated a comparable association between surface N_2O emissions and elevated N_2O concentrations in the top soil layer of 0–15 cm in a cotton field. In our study, up to 52% of the variation of the data was explained by the regression models for N_2 and N_2O (Fig. 5a, b). Additionally, the statistical significance of the N_2 regression models was stronger than for N_2O.

The observed spatiotemporal dynamics of measured vertical δ^{15}N patterns in N_2 generally support the observed temporal dynamics of N_2 measurements. This encourages the development and testing of new methods to better constrain field N_2 emissions based on in situ sampling of soil N gases. E.g., in future applications, our data could serve to validate $^{15}N_2$ diffusion modelling approaches targeted to constrain underestimation of denitrification by ^{15}N subsoil diffusion and storage (Well et al. 2019b). Furthermore, the gradient method, considering diffusivity (Maier and Schack-Kirchner 2014), could be used to derive vertical fluxes of N_2 to be compared with chamber fluxes, at least when N_2 sources are not too close to the soil surface so that a relevant enrichment gradient can form. Given that the detection limit for denitrification is lower in soil air compared to chamber fluxes, soil air δ^{15}N analyses, including analyses of soil air N_2:N_2O product ratios might serve to reveal sound flux estimates in phases when chamber fluxes are below the detection limit. In this context, the presented dataset is an excellent prerequisite for developing and testing such a potential new method to assess field N_2 emissions based on in situ sampling of soil N gases.

Conclusions

This study provides a unique combination of field N_2 flux measurements and lysimeter-based ^{15}N fertilizer mass balances, thereby successfully demonstrating that the ^{15}NGF method delivers realistic estimates of N_2 flux under field conditions in ambient atmosphere. The soil air $\delta^{15}N_2$ data, along with the profile data of environmental controls of denitrification, further support the trustworthiness of measured N_2 emissions at the soil-atmosphere interface. Additionally, these findings suggest that combining such measurements with soil gas diffusion modeling and the gradient method could offer an alternative approach to constrain soil N_2 emissions. With its high temporal resolution of environmental data, encompassing all key components of the N cycle in a winter wheat rotation, we present a benchmark dataset for testing process-based biogeochemical ecosystem models. Furthermore, the successful cross-comparison of the ^{15}NGF method with the ^{15}N mass balance approach calls for a broader application of the ^{15}NGF method across various agricultural ecosystems in order to create more reliable N_2 emission data as a solid basis for the development of strategies to mitigate N losses from agriculture.

Supplementary Information The online version contains supplementary material available at https://doi.org/10.1007/s00374-024-01801-4.

Acknowledgements This work was supported by the German Science Foundation (DFG) with the research unit DASIM. Further support was obtained from the Helmholtz TERENO initiative. The authors would like to express their sincere gratitude to Elisabeth Ramm, Anja Schäfler-Schmid, Allison Kolar, Gwendolyn Schumacher, Joshua Braun-Wimmer, Nataliia Hordovska, and Elizabeth Wangari for their invaluable assistance with the field measurements, sampling and laboratory analyses. The authors acknowledge their contributions with great appreciation.

Funding This study was funded by the German Research Foundation (DFG) within the research unit DASIM.
Open Access funding enabled and organized by Projekt DEAL.

Declarations

Competing interests The authors have no relevant financial or non-financial interests to disclose. The authors have no competing interests to declare that are relevant to the content of this article. All authors certify that they have no affiliations with or involvement in any organization or entity with any financial interest or non-financial interest in the subject matter or materials discussed in this manuscript. The authors have no financial or proprietary interests in any material discussed in this article.

References

Anas M, Liao F, Verma KK, Sarwar MA, Mahmood A, Chen ZL, Li Q, Zeng XP, Liu Y, Li YR (2020) Fate of nitrogen in agriculture and environment: agronomic, eco-physiological and molecular approaches to improve nitrogen use efficiency. Biol Res 53:47

Arah JRM (1992) New formulae for mass spectrometric analysis of nitrous oxide and dinitrogen emissions. Soil Sci Soc Am J 56:795–800

Aulakh MS, Doran JW, Mosier AR (1991) Field evaluation of four methods for measuring denitrification. Soil Sci Soc Am J 55:1332–1338

Baily A, Watson CJ, Laughlin R, Matthews D, McGeough K, Jordan P (2012) Use of the N gas flux Method Measure Source Level N2O N2 Emissions Grazed Grassland Nutr Cycl Agroecosyst 94:287–298

Barton L, McLay CDA, Schipper LA, Smith CT (1999) Annual denitrification rates in agricultural and forest soils: a review. Soil Res 37:1073–1094. https://doi.org/10.1071/SR99009

Bayerisches Staatsministerium für Ernährung, Landwirtschaft und Forsten (2021) Winterweizen – Aktuelle Ergebnisse aus der Praxis und den Landessortenversuchen. Retrieved from https://www.lfl.bayern.de/ipz/getreide/226651/index.php. Accessed 31 Aug. 2021

Bergsma TT, Ostrom NE, Emmons M, Robertson GP (2001) Measuring simultaneous fluxes from soil of N. Technique Environ Sci Technol 35:4307–4312

Buchen C, Lewicka-Szczebak D, Fuß R, Helfrich M, Flessa H, Well R (2016) Fluxes of N. N2O Contributing Processes Summer after Grassland Renew Grassland Convers Maize Cropping Plaggic Anthrosol Histic Gleysol Soil Biol Biochem 101:6–19

Buchen-Tschiskale C, Well R, Flessa H (2023) Tracing nitrogen transformations during spring development of winter wheat induced by. Sci Total Environ 871:162061

Butterbach-Bahl K, Willibald G, Papen H (2002) Soil core method for direct simultaneous determination of N. N2O Emissions for Soils Plant Soil 240:105–116

Butterbach-Bahl K, Baggs EM, Dannenmann M, Kiese R, Zechmeister-Boltenstern S (2013) Nitrous oxide emissions from soils: how well do we understand the processes and their controls? Philos Trans R Soc B: Biol Sci 368:20130122

Cárdenas LM, Hawkins JMB, Chadwick D, Scholefield D (2003) Biogenic gas emissions from soils measured using a new automated laboratory incubation system. Soil Biol Biochem 35:867–870

Čuhel J, Šimek M, Laughlin RJ, Bru D, Chèneby D, Watson CJ, Philippot L (2010) Insights into the effect of soil pH on N. Emissions Denitrifier Community Size Activity Appl Environ Microbiol 76:1870–1878. https://doi.org/10.1128/AEM.02484-09

Dannenmann M, Bimüller C, Gschwendtner S, Leberecht M, Tejedor J, Bilela S, Gasche R, Hanewinkel M, Baltensweiler A, Kögel-Knabner I, Polle A, Schloter M, Simon J, Rennenberg H (2016) Climate Change impairs Nitrogen Cycling in European Beech forests. PLoS ONE 11:e0158823

Davidson EA, Kanter D (2014) Environ Res Lett 9:105012

Friedl J, Cardenas LM, Clough TJ, Dannenmann M, Hu C, Scheer C (2020) Measuring denitrification and the N. Curr Opin Environ Sustain 47:61–71

Friedl J, Warner D, Wang W, Rowlings DW, Grace PR, Scheer C (2023) Strategies for mitigating N. Emissions Intensive Sugarcane Cropping Syst Nutr Cycl Agroecosyst 125:295–308

Fu J, Gasche R, Wang N, Lu H, Butterbach-Bahl K, Kiese R (2017) Impacts of climate and management on water balance and nitrogen leaching from montane grassland soils of S-Germany. Environ Pollut 229:119–131

Galloway JN, Cowling EB (2002) Reactive Nitrogen and the World: 200 years of change. Ambio 31:64–71

Groffman P, Altabet M, Bohlke J, Butterbach-Bahl K, David M, Firestone M, Giblin A, Kana T, Nielsen LP, Voytek M (2007) Methods for measuring denitrification: diverse approaches to a difficult problem. Ecol Appl 16:2091–2122

Jantalia C, Halvorson A, Follett R, Alves B, Polidoro J, Urquiaga S (2012) Nitrogen source effects on ammonia volatilization as measured with Semi-static Chambers. Agron J 104:1595

Kempers AJ, Zweers A (1986) Ammonium determination in soil extracts by the salicylate method. Commun Soil Sci Plant Anal 17:715–723

Kiese R, Fersch B, Baessler C, Brosy C, Butterbach-Bahl K, Chwala C, Dannenmann M, Fu J, Gasche R, Grote R, Jahn C, Klatt J, Kunstmann H, Mauder M, Rödiger T, Smiatek G, Soltani M, Steinbrecher R, Völksch I, Schmid HP (2018) The TERENO Pre-alpine observatory: integrating meteorological, hydrological, and biogeochemical measurements and modeling. Vadose Zone J 17:1–17

Kulkarni MV, Burgin AJ, Groffman PM, Yavitt JB (2014) Direct flux and. Biogeochemistry 117:359–373

Li Y, Gao X, Tenuta M, Gui D, Li X, Zeng F (2021) Linking soil profile N. Environ Pollut 285:117458

Lindau CW, Patrick WH, Delaune RD, Reddy KR (1990) Rate of accumulation and emission of N. N2O CH4 Flooded rice soil Plant Soil 129:269–276

Liu Y, Wang R, Pan Z, Zheng X, Wei H, Zhang H, Mei B, Quan Z (2022) Quantifying in situ N. fluxes intensively managed calcareous soil using 15 N gas-flux method J Integr Agric 21:2750–2766. https://doi.org/10.1016/j.jia.2022.07.016

Ma L, Janz B, Kiese R, Mwanake R, Wangari E, Butterbach-Bahl K (2021a) Effect of vole bioturbation on N. NO NH3 CH4 CO2 Fluxes Slurry Fertilized non-fertilized Montane grassland soils South Ger Sci Total Environ 800:149597

Ma R, Zou J, Han Z, Yu K, Wu S, Li Z, Liu S, Niu S, Horwath WR, Zhu-Barker X (2021b) Global soil-derived ammonia emissions from agricultural nitrogen fertilizer application: a refinement based on regional and crop-specific emission factors. Glob Change Biol 27:855–867

Maier M, Schack-Kirchner H (2014) Using the gradient method to determine soil gas flux: a review. Agric Meteorol 192–193:78–95

Malone JP, Stevens RJ, Laughlin RJ (1998) Combining the. Soil Biol Biochem 30:31–37

Mathivanan GP, Eysholdt M, Zinnbauer M, Rösemann C, Fuß R (2021) New N. Agric Ecosyst Environ 322:107640

Micucci G, Sgouridis F, McNamara NP, Krause S, Lynch I, Roos F, Well R, Ullah S (2023) The. Curr Progress Future Dir Soil Biol Biochem 184:109108

Mosier AR, Klemedtsson L (1994) Measuring denitrification in the field. In: Weaver RW, Angle JS, Bottomley PS (eds) Methods of Soil Analysis. Microbiol Biol Prop, vol 2. SSSA, Madison, Wis., pp 1047–1065

Mosier AR, Guenzi WD, Schweizer EE (1986a) Field Denitrification Estimation by Nitrogen-15 and acetylene inhibition techniques. Soil Sci Soc Am J 50:831–833
Mosier AR, Guenzi WD, Schweizer EE (1986b) Soil losses of Dinitrogen and Nitrous Oxide from Irrigated crops in Northeastern Colorado. Soil Sci Soc Am J 50:344–348
Mosier AR, Chapman SL, Freney JR (1989) Determination of dinitrogen emission and retention in floodwater and porewater of a lowland rice field fertilized with. Fertil Res 19:127–136
Mulvaney RL (1984) Determination of. Soil Sci Soc Am J 48:690–692
Mulvaney RL, Kurtz LT (1984) Evolution of Dinitrogen and Nitrous Oxide from Nitrogen-15 fertilized soil cores subjected to wetting and drying cycles. Soil Sci Soc Am J 48:596–602
Myrold DD (1990) Measuring denitrification in soils using. In: Revsbech NP, Sorensen J (eds) Denitrification in soil and sediment. Plenum: New York London. 181–198
Origin(Pro) (2020) OriginLab Corporation, Northampton, MA, USA
Pai SC, Su YT, Lu MC, Chou Y, Ho TY (2021) Determination of Nitrate in Natural Waters by Vanadium reduction and the Griess assay: reassessment and optimization. ACS ESandT Water 1:1524–1532
Pan Z, Wang R, Liu Y, Wang L, Zheng X, Yao Z, He Z, Zhang X (2022a) Characteristics of N_2 and N2O Fluxes Cultivated Black Soil: Case Study Through Situ Meas Using 15 N Gas Flux Method Agric 12:1664
Pan B, Xia L, Lam SK, Wang E, Zhang Y, Mosier A, Chen D (2022b) A global synthesis of soil denitrification: driving factors and mitigation strategies. Agric Ecosyst Environ 327:107850
Parkin TB (1987) Soil microsites as a source of Denitrification Variability. Soil Sci Soc Am J 51:1194–1199
Pütz T, Kiese R, Wollschläger U, Groh J, Rupp H, Zacharias S, Priesack E, Gerke HH, Gasche R, Bens O, Borg E, Baessler C, Kaiser K, Herbrich M, Munch JC, Sommer M, Vogel HJ, Vanderborght J, Vereecken H (2016) TERENO-SOILCan: a lysimeter-network in Germany observing soil processes and plant diversity influenced by climate change. Environ Earth Sci 75:1242
Qasim W, Zhao Y, Wan L, Lv H, Lin S, Gettel GM, Butterbach-Bahl K (2022) The potential importance of soil denitrification as a major N loss pathway in intensive greenhouse vegetable production systems. Plant Soil 471:157–174
R Core Team (2019) R: a language and environment for statistical computing. R Foundation for Statistical Computing, Vienna
Ravishankara AR, Daniel JS, Portmann RW (2009) Nitrous Oxide (N. Dominant Ozone-Depleting Subst Emitted 21st Century Sci 326:123–125
Rehschuh S, Fuchs M, Tejedor J, Schäfler-Schmid A, Magh R-K, Burzlaff T, Rennenberg H, Dannenmann M (2019) Admixing fir to European Beech forests improves the Soil Greenhouse Gas Balance. Forests 10:213
Rethemeyer J (2004) Organic carbon transformation in agricultural soils: radiocarbon analysis of organic matter fractions and biomarker compounds. Dissertation, Christian-Albrechts-Universität, Kiel
Rohe L, Apelt B, Vogel HJ, Well R, Wu GM, Schlüter S (2021) Denitrification in soil as a function of oxygen supply and demand at the microscale. Biogeosciences 18:1185–1201
Rolston DE, Hoffman DL, Toy DW (1978) Field Measurement of Denitrification: I. Flux of N. N2O Soil Sci Soc Am J 42:863–869
Rolston DE, Broadbent FE, Goldhamer DA (1979) Field Measurement of Denitrification: II. Mass Balance and Sampling uncertainty. Soil Sci Soc Am J 43:703–708
Scheer C, Fuchs K, Pelster DE, Butterbach-Bahl K (2020) Estimating global terrestrial denitrification from measured N. Curr Opin Environ Sustain 47:72–80
Senbayram M, Well R, Shan J, Bol R, Burkart S, Jones DL, Wu D (2020) Rhizosphere processes in nitrate-rich barley soil tripled both N. Losses due Enhanced Bacterial Fungal Denitrification Plant Soil 448:509–522
Sgouridis F, Stott A, Ullah S (2016) Application of the. N2O Fluxes due Denitrification Nat semi-natural Terr Ecosyst Comparison Acetylene Inhib Technique Biogeosciences 13:1821–1835
Siegel RS, Hauck RD, Kurtz LT (1982) Determination of. Application Meas N2 Evol Dur Denitrification Soil Sci Soc Am J 46:68–74
Stevens RJ, Laughlin RJ (2001) Lowering the detection limit for dinitrogen using the enrichment of nitrous oxide. Soil Biol Biochem 33:1287–1289
Takeda N, Friedl J, Kirkby R, Rowlings D, Scheer C, De Rosa D, Grace P (2023) Denitrification losses in response to N fertiliser rates - a synthesis of high temporal resolution N. in-situ 15N2O 15N2 measurements fertiliser 15 N recoveries intensive sugarcane Syst Biogeosciences 128:2169–8953
Tauchnitz N, Spott O, Russow R, Bernsdorf S, Glaser B, Meissner R (2015) Release of nitrous oxide and dinitrogen from a transition bog under drained and rewetted conditions due to denitrification: results from a. Isot Environ Health Stud 51:300–321
Tenspolde A, Kleineidam K, Müller C, Wrage-Mönnig N (2023) Application of isotopic labels optimized for large scale plot experiments. Biol Fertil Soils. https://doi.org/10.1007/s00374-023-01730-8
Vanden Heuvel RM, Mulvaney RL, Hoeft RG (1988) Evaluation of Nitrogen-15 Tracer techniques for direct measurement of Denitrification in Soil: II. Simulation studies. Soil Sci Soc Am J 52:1322–1326
Warner DI, Scheer C, Friedl J, Rowlings DW, Brunk C, Grace PR (2019) Mobile continuous-flow isotope-ratio mass spectrometer system for automated measurements of N2 and N2O fluxes in fertilized cropping systems. Sci Rep 9:11097. https://doi.org/10.1038/s41598-019-47451-7
Well R, Butterbach-Bahl K (2013) Comments on A test of a field-based 15 N-nitrous oxide pool dilution technique to measure gross N2O production in soil by Yang (2011), Global Change Biology 17:3577–3588. Global Change Biology 19:133–135. https://doi.org/10.1111/gcb.12005
Well R, Burkart S, Giesemann A, Grosz B, Köster JR, Lewicka-Szczebak D (2019a) Improvement of the. Rapid Commun Mass Spectrom 33:437–448
Well R, Maier M, Lewicka-Szczebak D, Köster J-R, Ruoss N (2019b) Underestimation of denitrification rates from field application of the. Biogeosciences 16:2233–2246
Wen Y, Chen Z, Dannenmann M, Carminati A, Willibald G, Kiese R, Wolf B, Veldkamp E, Butterbach-Bahl K, Corre MD (2016) Disentangling gross N. Sci Rep 6:36517
Westhoek H, Lesschen JP, Leip A, Rood T, Wagner S, De Marco A, Murphy-Bokern D, Pallière C, Howard CM, Oenema O, Sutton MA (2015) Nitrogen on the table: the influence of food choices on nitrogen emissions and the European environment. (European Nitrogen Assessment special report on nitrogen and food). Centre for Ecology & Hydrology. https://edepot.wur.nl/368693
Wolf B, Zheng X, Brüggemann N, Chen W, Dannenmann M, Han X, Sutton MA, Wu H, Yao Z, Butterbach-Bahl K (2010) Grazing-induced reduction of natural nitrous oxide release from continental steppe. Nature 464:881–884
Wolf B, Chen W, Brüggemann N, Zheng X, Pumpanen J, Butterbach-Bahl K (2011) Applicability of the soil gradient method for estimating soil–atmosphere CO. CH4 N2O Fluxes Steppe Soils Inner Mongolia J Plant Nutr Soil Sci 174:359–372
Wu H, Dannenmann M, Fanselow N, Wolf B, Yao Z, Wu X, Brüggemann N, Zheng X, Han X, Dittert K, Butterbach-Bahl K (2011) Feedback of grazing on gross rates of N mineralization and inorganic N partitioning in steppe soils of Inner Mongolia. Plant Soil 340:127–139
Yang WH, Teh YA, Silver WL (2011) A test of a field-based. Glob Change Biol 17:3577–3588

Zhang C, Xiaotang J, Jinbo Z, Rees RM, Müller C (2023) Soil PH and Long-Term Fertilization Affect Gross N Transformation and N. Biol Fertil Soils 59:527–539

Zheng J, Zhou M, Zhu B, Fan J, Lin H, Ren B, Zhang F (2023) Drip fertigation sustains crop productivity while mitigating reactive nitrogen losses in Chinese agricultural systems: evidence from a meta-analysis. Sci Total Environ 886:163804

Zistl-Schlingmann M, Feng J, Kiese R, Stephan R, Zuazo P, Willibald G, Wang C, Butterbach-Bahl K, Dannenmann M (2019) Dinitrogen emissions: an overlooked key component of the N balance of montane grasslands. Biogeochem 143:15–30

Zistl-Schlingmann M, Kwatcho Kengdo S, Kiese R, Dannenmann M (2020) Management Intensity Controls Nitrogen-Use-Efficiency and flows in Grasslands—A 15 N Tracing Experiment. Agronomy 10:106. https://doi.org/10.3390/agronomy10040606